APPLICATIONS OF PERPENDICULAR-TO-GRAIN COMPRESSION BEHAVIOR IN REAL WOOD CONSTRUCTION ASSEMBLIES

Craig T. Basta

Former Graduate Research Assistant
E-mail: craig.basta@oregonstate.edu

Rakesh Gupta†

Professor
Department of Wood Science and Engineering
Oregon State University
Corvallis, OR 97331
E-mail: rakesh.gupta@oregonstate.edu

Robert J. Leichti

Product Compliance Manager, Hand Tools & Fasteners
Stanley Black&Decker
Briggs Drive East Greenwich, RI 02888
E-mail: rleichti@stanleyworks.com

Arijit Sinha*†

Assistant Professor
234 Richardson Hall
Department of Wood Science and Engineering
Oregon State University
Corvallis, OR 97331
E-mail: Arijit.sinha@oregonstate.edu

Abstract. Compression perpendicular to grain ($C_\perp$) of wood is an important property and has a drastic effect on serviceability of the structure. Typical $C_\perp$ loading scenarios include the bottom chord of a truss resting on the top plate of a shear wall and chords of a shear wall resting on the bottom plate. Present design values for $C_\perp$ are based on stress at 1-mm deflection for an ASTM block test. However, in real applications, loading conditions and deflection limits are much different from that administered during the test. There is a need to characterize $C_\perp$ behavior of wood in construction applications and compare it with current design codes. This study addresses that by testing two different assemblies involving $C_\perp$ loading, each with two different species of wood, to quantify the design $C_\perp$ based on the desired application and compare it with current design codes. Also, the effect of species and aspect ratio of assembly was characterized. Results suggested that the ASTM values significantly differ from the assembly values. Species of wood did not have any effect on the performance of the assemblies. A 2% strain offset method was proposed to determine allowable value for $C_\perp$ for a desired application. Adjustment factors based on loading configurations were suggested for calculation of design values.

Keywords: Construction applications, $C_\perp$ design, shear walls, wood-frame truss, wood-on-wood bearing.

INTRODUCTION

In modern wood-frame construction, compression perpendicular to grain ($C_\perp$) of wood is an important property that seldom governs failure but has a drastic effect on serviceability of the structure. Typical $C_\perp$ loading scenarios include the bottom chord (BC) of a truss resting on the top plate (TP) of a shear wall and chords of shear wall resting on the bottom plate (BP). Despite

* Corresponding author
† SWST member

$C_\perp$ loading being quite common in a structure, its behavior in practical applications has not been characterized at all (Gehri 1997; Blass and Gorlacher 2004; Leijten et al 2010). Reference values for $C_\perp$ in the US design code, National Design Specifications (NDS), are based on tests that are not representative of actual loading scenarios and have arbitrary deflection limits (Gehri 1997; Basta et al 2011).

The common test used for $C_\perp$ in the US is a block compression test based on ASTM (2010a), in which load value at a deflection of 1 mm is the $C_\perp$ value (AFPA 2007). The standard has many limitations. The loading uses a metal block on a wood surface, whereas in structures, it is typically wood-on-wood contact (Fergus et al 1981). The metal block is 50×50 mm and does not cover the whole surface of the wood. The behavior of wood is different when the block is loaded entirely or partially (Blass and Gorlacher 2004). Because of partial covering of the wood specimen by the metal block, shear stresses as well as compressive stresses are developed. Shear stresses with corresponding reactions, which develop at the edges of the bearing plate, lead to higher $C_\perp$ values than if load was applied across the full area of the specimen (Kunesh 1968; Bodig 1969; Pellicane et al 1994a). The metal block does have the purpose of ensuring the test results represent compression values for a single element (wood specimen) and minimize interference of the loading assembly.

A point of discussion has been if the standards should aim at getting well-defined basic material properties or reflect typical uses. $C_\perp$ is dependent on loading geometry, specimen geometry, and material properties of wood. Stress distributions in wood members subjected to $C_\perp$ loading were complex, even with load applied across the entire surface of wood material (Pellicane et al 1994b). Because of the complexity, large shear forces existed close to the edges of loading plates (Pellicane et al 1994a), but shearing failure did not generally occur before 1 mm of deformation (Fergus et al 1981). Additionally, $C_\perp$ load-carrying capacity of wood increased with increasing edge-to-surface ratio of loading plates (Bodig 1969).

Wood-on-wood compression reached a maximum stress of 68-85% of metal-on-wood (ASTM) compression (Fergus et al 1981). Johnson (1983) compared Hem-fir and Douglas-fir (DF) specimens in $C_\perp$ and found DF specimens were 150% as strong in $C_\perp$ as Hem-Fir specimens of corresponding grade mainly because of its dense grain structure.

The deflection of 1 mm, specified by the NDS (AFPA 2007), at which compressive stress has to be measured, is an arbitrary value. It is an acceptable value when the aspect ratio (height/width) is 1 or less. In structures, higher deflection values are acceptable without violating the serviceability limit state (Leijten et al 2010). Deflection limits vary with depth of the structural member. It is quite difficult to understand why exceeding the deformation limit in a block compression is the governing criteria for structures in which much larger deformations are normally acceptable and the loading configuration is different. Previous research has not attempted to characterize behavior or test assemblies that represent real-world scenarios. Most of the research has concentrated on single elements, such as solid wood (Johnson 1983; Gehri 1997; Leijten et al 2010) and glulams (Damkilde et al 2000). Research on wood connections with wood-to-wood contact, eg mortise and tenon joints, has focused on calculating compression of each element separately and then combining to predict connection behavior (Schmidt and Daniels 1999). Therefore, studying representative assemblies under compression loading is important for increasing our understanding of wood-to-wood contact in compression.

In typical uses, $C_\perp$ presents some design limiting concerns, especially in the trusses (Fergus et al 1981; Lum and Varoglue 1988). An experimental full-scale truss failed at 1.94 times design load because of perpendicular-to-grain wood crushing at the right support, showing excessive deformation (Lum and Varoglue 1988). This design load ratio of 1.94 was significantly lower than the 3.0-6.0 range reported in the literature (Wolfe et al 1986). This failure caused by perpendicular-to-grain wood crushing further emphasizes the need for characterizing perpendicular-to-grain

behavior of representative assemblies with wood-to-wood contact. There is a case for and a debate on increasing allowable $C_\perp$ values using typical application test results. Bulmanis et al (1983) addressed the issue of increasing allowable transverse compression stress at the interface of wood-bearing members by focusing on the bearing connection of the BC of a truss member on the TP of the supporting wall. Locating the truss plate at the lower bottom edge of the BC in such a manner that compression stress is distributed to the vertical faces of the BC led to a 15% increase in compression strength, which was calculated from load at proportional limit. Similarly, Lum and Karacabeyli (1994) justified a 15% increase in allowable stress, $F_{c\perp}$, for flatwise loading by experimental and analytical studies. They also recognized that $C_\perp$ loads on opposite sides of a member and near the longitudinal end of a member are a more severe loading case than single side loading across the central area. This resulted in a 66% decrease in $C_\perp$ loads for load applied to opposite sides of a member near the longitudinal end (Lum and Karacabeyli 1994). Both adjustments are now included in the Canadian code. However, the US design code (NDS) does not address this issue (AFPA 2007). The NDS does allow for an increase in allowable $F_{c\perp}$ values through the bearing area factor C_b. Bearing stress is applied because of two members in contact, and the factor accounts for strength provided by adjacent material. C_b is dependent on contact length between two members and ranges between 1.75-1.0 (AFPA 2007). Comparatively, in Europe, a design approach was suggested in which a characteristic value for $C_\perp$ is based on full surface compression (Blass and Gorlacher 2004). This characteristic value was further adjusted for effective contact length parallel to grain. If the timber member under compression protrudes past the contact area, effective contact length may be increased and correspondingly effective area increased. Also, this design approach proposes to distinguish between ultimate limit and serviceability states.

There is a pressing need to characterize $C_\perp$ value for real application scenarios involving wood-on-

wood compression. This study proposes a method to determine $C_\perp$ strength from tested assemblies. The objectives of this study are to:

1. determine appropriate criteria for $C_\perp$ strength in test assemblies,
2. determine influence of wood species within test assemblies, and
3. quantify the relationship between aspect ratio and $C_\perp$ behavior including ultimate limit state within tested assemblies by
   (a) comparing $C_\perp$ strength for BC of truss assemblies across a range of aspect ratios, and
   (b) quantifying maximum stress and strain at maximum stress in high aspect ratio members.

MATERIALS AND METHODS

Two very common $C_\perp$ construction assemblies were tested. Figure 1 is a schematic of the two types of assemblies. The first assembly (Fig 1a) represents a BC of truss on TP of wall (BC assembly). The member representative of the BC truss is referred to as the BC member, and the member representing the TP of the wall is referred to as the TP member. The longitudinal end of the BC member was sandwiched between the TP members (Fig 1a). Three different DF BC members were used with thicknesses of 89 mm (2 × 4), 184 mm (2 × 8), and 292 mm (2 × 12). In BC-Spruce-Pine-Fir (SPF) assemblies, the TP members were SPF and the BC member was DF. The lower TP member rested on a rigid metal plate, and the load was applied through a metal plate to the surface of TP members. In BC assemblies, four main conditions apply. First, load was applied through a metal plate to the full surface on one wide face and wood-on-wood partial surface compression on the other wide face of the TP member (Fig 1b). This condition is similar to the ASTM test specimen. Second, both narrow faces of the longitudinal end of the BC member were loaded (Fig 1a). The ASTM specimen does not represent this condition. Third, bearing is through wood-to-wood contact as opposed to metal-on-wood for the ASTM specimen. Fourth, aspect ratio of
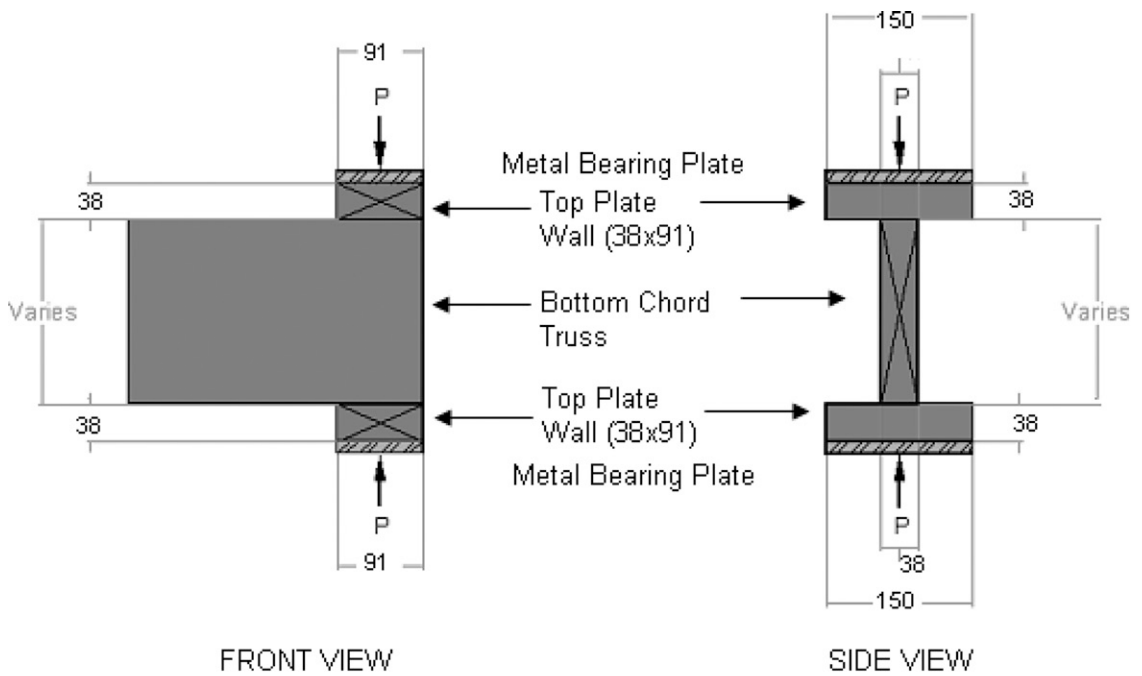
(a) BC assembly schematic-truss bottom chord on wall top plate
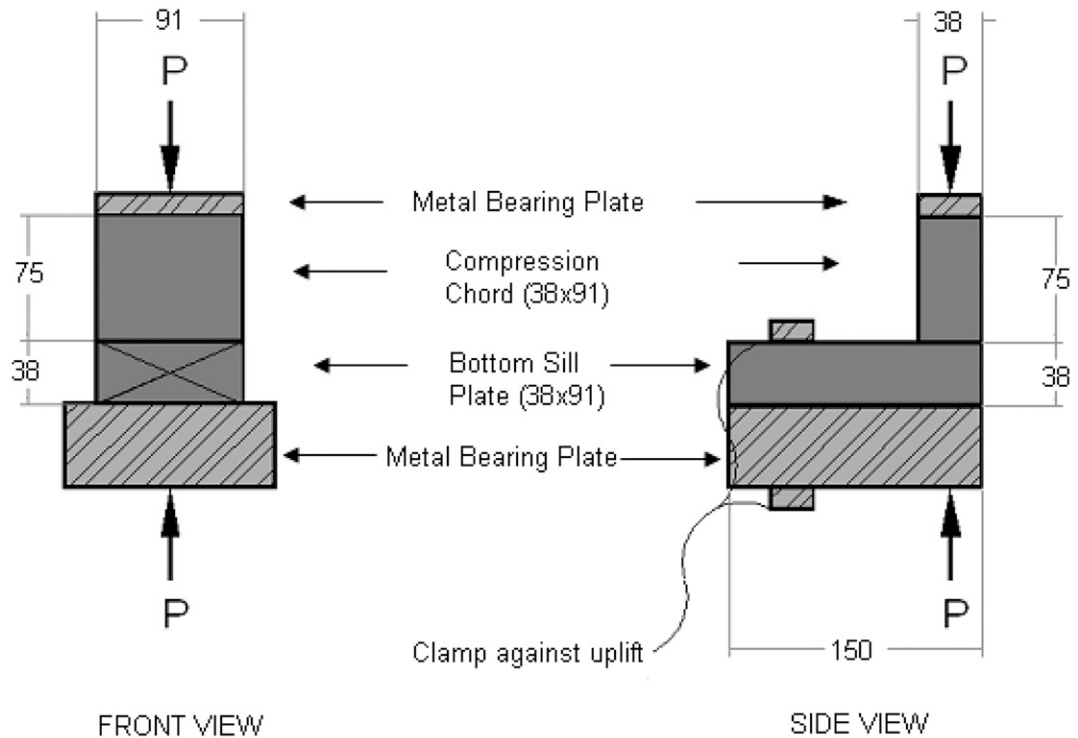
(b) BC assembly schematic-compression chord bearing on bottom plate of wall.

Figure 1.   Schematics of bottom plate (BP) and bottom chord (BC) assemblies.

the BC member varies (2.3 for 2 × 4, 4.8 for 2 × 8, and 7.5 for 2 × y 12) as opposed to aspect ratio of 1 for the ASTM specimen.

The second assembly represented a compression chord (CC) of a shear wall on the BP of a wall (BP assembly) (Fig 1b). In this assembly, a longitudinal CC member of a shear wall rests on the wide face of the wall BP. CC members were 75-mm-long 38 × 89 mm (nominal 2 × 4) DF members, whereas BP members were 150 mm long, 38 × 89 mm and were either DF or SPF. The BP member rested on a metal plate, and the load was applied through a metal plate on the top surface of the CC member. As a result, load was applied to the BP member through wood-on-wood contact by the longitudinally loaded CC member. Both wide faces of the longitudinal end of the BP member were stressed (Fig 1b). This condition is not represented by the ASTM specimen. The sill plate was fastened to the bottom surface to prevent vertical movement and rotation (Fig 2). Also, for each BC and BP assembly, from the constituting materials from each of the assemblies, ASTM specimens were also tested. The numbers of samples tested in assembly and ASTM specimens are listed in the test matrix (Table 1).

MATERIALS

SPF and DF materials were obtained from Action Wood Products (Turner, OR). Boards were grouped by species and dimension. Boards in each group were randomly assigned to assemblies BC or BP and then cut to fabricate assemblies. When possible, defect-free, or close to defect-free, samples were cut from wood material, ie an effort was made to cut around knots, wane, and other defects in the boards. When defects were present, samples were arranged during testing to minimize their effect. Samples were cut in a fashion deemed to be consistent with construction practice. Contact surfaces were rough, and members were not always perfectly rectilinear. Prior to testing, all specimens were conditioned at 20°C and 65% humidity until daily weight became stable. Member dimensions (length, width, and thickness) were measured.
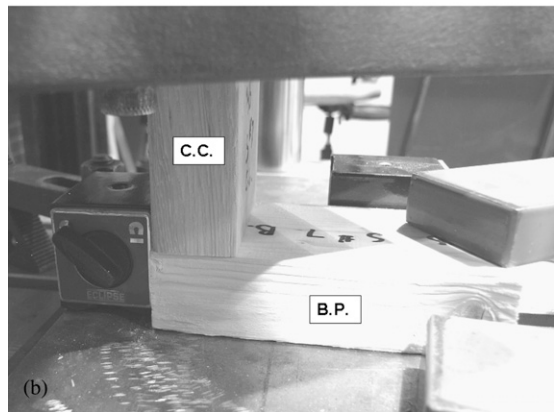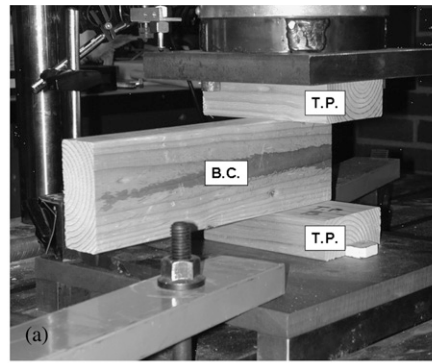

Figure 2. Test set up of (a) bottom chord (BC) assembly and (b) bottom plate (BP) assembly.

Data recorded for each sample included rings/mm, percentage latewood, and average ring angle with respect to load. Specific gravity of the material was calculated as per ASTM (2010b). These data were used as covariates in analysis of variance (ANOVA) statistical analyses (Ramsey and Schafer 2002).

Test Set-Up

The test set-up for BC and BP assemblies is shown in Fig 2a and b, respectively. To test the specimen, a Universal testing machine comprised of an MTS hydraulic actuator was used. In the BC assembly (Fig 2a), the lower TP rested on a metal plate and was held in position using magnetic stops. The test head was brought flush with the upper TP member, and the truss BC and

Table 1.   Test matrix (all dimension in mm).[a]

Bottom chord (BC) of truss on top plate (TP) of wall (BC assembly)							
BC of truss, Douglas-fir (DF)		TP of wall	TP species	Symbol	No. of samples (n)		Loading rate (mm/min)	
					Assembly	ASTM of BC member (DF)	Initial	Post 10% strain
38×89	(2×4)	38×89	Douglas-fir	BC-2 × 4 DF	20	20	3.3	33
			Spruce-Pine-Fir	BC-2 × 4 SPF	20			
38×184	(2×8)	38×89	Douglas-fir	BC-2 × 8 DF	17	20	5	26
			Spruce-Pine-Fir	BC-2 × 8 SPF	18			
38×292	(2×12)	38×89	Douglas-fir	BC-2 × 12 DF	20	20	7.2	7.2
			Spruce-Pine-Fir	BC-2 × 12 SPF	20			
Compression chord (CC) of truss on top plate of wall (BP assembly)							
BP		CC of wall, DF	Species of BP	Symbol	No. of samples (n)		Loading rate (mm/min)	
					Assembly	ASTM of BP member	Initial	Post 10% strain
38×89	(2×4)	38×89	Douglas-fir	BP-DF	20	20	0.762	7.6
38×89	(2×4)		Spruce-Pine-Fir	BP-SPF	10	10		

[a] Loading rate for all ASTM specimen = 0.762 mm/min.

upper TP were positioned (or brought to a zero deflection point). This minimized initial effects in the tests. In the BP assembly (Fig 2b), the BP member rested on the metallic base plate. Magnetic stops were used to hold the CC and BP members in their respective positions. The CC could translate only vertically.

Total assembly deflection was measured by an LVDT connected to a National Instrument data acquisition system, and this deflection was correlated to cross head displacement. Compression force was recorded by the load cell mounted on the actuator. Loading deflection rates for various assemblies are listed in Table 1. Two different loading rates were used for each assembly, initial and post 10% compressive strain, respectively. Testing was continued until the assembly showed severe member deformations and were deemed failed. Loading rate for each assembly type differed (Table 1) to maintain a constant initial system strain rate of 0.02 per minute.

ASTM specimens were tested according to guidelines established in ASTM D-143 for $C_\perp$ testing with the following exceptions: depth measured to only 38 mm because of use of standard dimensional lumber, ring angle with respect to applied load was not controlled, and testing was conducted at a constant cross head displacement rate of 0.76 mm/min. Load and compressive deflection were recorded throughout testing.

Data Analysis

The linear range in the stress–strain diagrams was identified by visual inspection. Stress offsets were defined by means of a linear regression for data fitting. Offset load is defined as the intersection of load–deformation (P-Δ) curve and a line parallel to the initial linear portion of the P-Δ curve offset by the requisite amount in the positive direction. The wood-to-wood bearing results in large initial portions of misalignment that do not represent true behavior but are a testing artifact. Consequently, it is important to offset the values by a definite amount. For example, to calculate 2% offset stress, first a linear regression is fitted to the linear range on the stress–strain diagram. The regression is then extended back to zero stress. A 2% offset strain was calculated from strain at the intersection of the regression line with the strain axis. Both deflection and offset strain values reported are based on this approach. For all tests, stress values were recorded at 1 mm system deflection ($\sigma_{0.04\text{-}D}$), 1 mm system offset deflection ($\sigma_{0.04\text{-}OD}$), 2% system strain ($\sigma_{2\%\text{-}S}$), and 2% system offset strain ($\sigma_{2\%\text{-}OS}$). Also, maximum stress (σ_{max}) and strain at maximum stress (ε_{max}) were calculated. The σ_{max} was defined as maximum stress achieved between 0 and maximum system strain without exceeding 10% system strain. All catastrophic failures with corresponding system strains and stresses were recorded. All pairwise statistical

tests were accomplished using a Tukey-Cramer multiple comparison (Ramsey and Schafer 2002) using Splus 8.1 (Tibco Software Inc. 2008). All ANOVA models were also developed using Splus 8.1 (Tibco Software Inc. 2008), and the various covariates were accounted for as a split-block ANOVA with 20 blocks. Models were also analyzed with and without inclusion of covariance and then compared. The complete procedure and results of the statistical evaluation are documented in Basta (2005).

RESULTS AND DISCUSSION

Determination of Compressive Strength

The typical stress–strain diagram for the four types of assemblies and the ASTM sample tested is shown in Fig 3, which illustrates the extreme differences between behaviors of ASTM tests and BC and BP assemblies. Behavior of DF and SPF assemblies were very similar, therefore, for illustration purposes, only DF tests are depicted. The NDS (AFPA 2007) stipulates that stress at deflection of 1 mm (2% strain) should be used as the F_{cperp} value for the sample. Whereas 1-mm

deflection corresponds to 2% strain in the standard ASTM specimen, ASTM specimens in this study were 38 mm deep rather than 50 mm. Hence, the 1-mm deflection corresponded to 2.67% strain in specimens used in this study. This same deflection corresponded to a system strain of less than 0.3% in BC-2 × 12 assemblies. With respect to stress at 1-mm deflection ($\sigma_{0.04\text{-}D}$), we observed vast differences in stresses encountered by ASTM samples and BC and BP assemblies. For example, stress at 1-mm deflection for ASTM specimen was 6.5 MPa, whereas that for a 2 × 4 BC was 3.6 MPa. Member depth plays an important role in compressibility of the members. Therefore, to account for depth of assemblies and to homogenize comparisons across assemblies, it is necessary to base stress values on a specific strain. The 1-mm deflection benchmark of the ASTM test corresponds to 2% strain. Thus, stress at 2% strain ($\sigma_{2\%\text{-}S}$) should be used for comparisons among different testing configurations and assemblies.

A typical stress–strain curve for each of the assemblies tested and the ASTM specimen is given in Fig 3. Calculated mean stress values
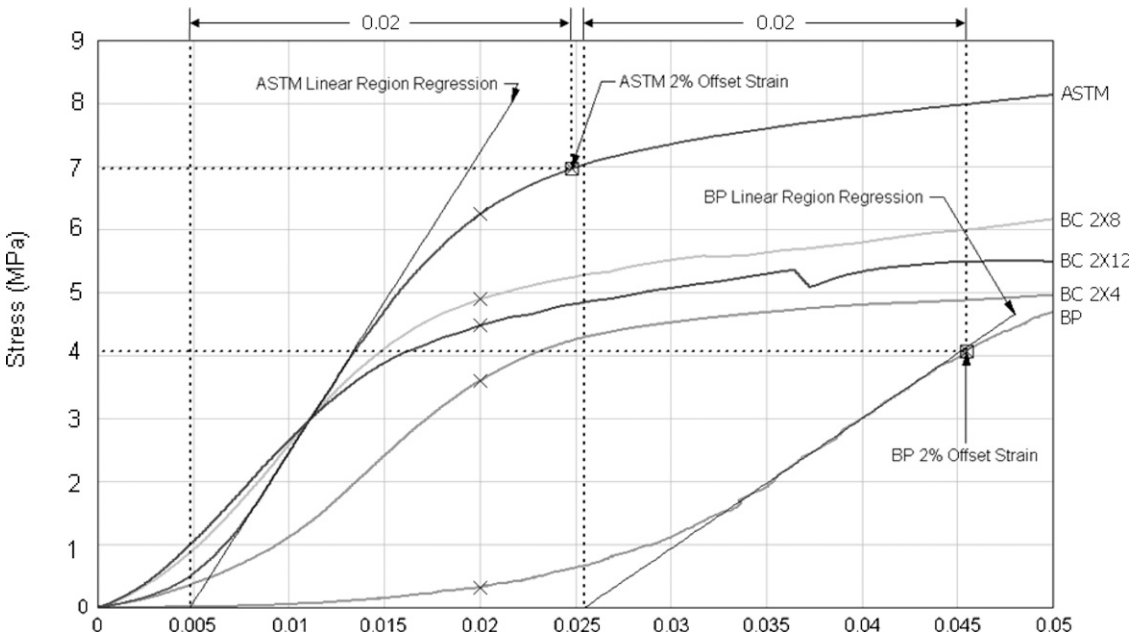

Figure 3.   Stress–strain diagram for ASTM samples and various assemblies.

Table 2. Stress (kPa) values at 1-mm deflection ($\sigma_{0.04\text{-}D}$), 1-mm offset deflection ($\sigma_{0.04\text{-}D}$), 2% system strain ($\sigma_{2\%\text{-}S}$), and 2% system offset strain ($\sigma_{2\%\text{-}S}$) along with their coefficient of variation (COV) in percent.

	Assemblies[a]	$\sigma_{0.04\text{-}D}$	COV	$\sigma_{2\%\text{-}S}$	COV	$\sigma_{0.04\text{-}OD}$	COV	$\sigma_{2\%\text{-}OS}$	COV
BC-2 × 4	BC-2 × 4 DF	862	45	4309	32	1951	34	4764	27
	BC-2 × 4 SPF	814	44	4102	21	1917	29	4495	22
	ASTM-2 × 4 DF	6647	22	5130	27	7260	24	6488	25
BC-2 × 8	BC-2 × 8 DF	531	35	4944	22	1393	25	5330	23
	BC-2 × 8 SPF	558	45	4578	22	1379	28	4944	18
	ASTM-2 × 8 DF	6357	35	4233	37	7950	31	6860	32
BC-2 × 12	BC-2 × 12 DF	421	46	4599	27	993	32	4826	26
	BC-2 × 12 SPF	379	48	4392	25	1014	32	4619	25
	ASTM-2 × 12 DF	5474	42	3854	51	7226	35	6143	35
BP	BP-DF	1034	34	531	99	5316	31	4426	34
	ASTM-2 × 4 DF	6702	22	5337	27	7260	24	6488	25
	BP-SPF	1737	59	841	62	4282	18	3503	21
	ASTM-2 × 4 SPF	5771	18	4640	33	6391	12	5874	16

[a] BC, bottom chord; DF, Douglas-fir; SPF, spruce-pine-fir; BP, bottom plate.

at all four deflection points, $\sigma_{0.04\text{-}D}$, $\sigma_{0.04\text{-}OD}$, $\sigma_{2\%\text{-}S}$, and $\sigma_{2\%\text{-}OS}$, are given in Table 2 along with their coefficients of variation (COV) for each assembly and their respective ASTM specimen. With the exception of the BP assembly, stress values are much closer to each other between testing configurations and geometries when based on stress at a specified system strain (Fig 3). The $\sigma_{2\%\text{-}S}$ for all BC assemblies combined, regardless of species used, were within 25% of each other. However, $\sigma_{2\%\text{-}S}$ for BP assemblies was very low because of the large initial misalignment region. The multiple wood member assemblies led to larger misalignment and settling effects than are present in standard ASTM tests. This led to correspondingly larger ranges of nonlinearity in the stress–strain diagram. There is a need to adjust for settlement effects in all assemblies. Also, initial misalignment does not represent true material behavior. Hence, it was deemed beneficial that an offset strain of 2% would be used for the majority of comparisons between testing configurations and assemblies. The 2% offset strain was calculated using the procedure described in the "Data Analysis" section. Comparing BP and ASTM, average offset strain values for DF and SPF ASTM specimens were 0.005 and 0.007, respectively. Average offset values for BP-DF and BP-SPF members were 0.027 and 0.022, respectively. For the BP assembly (Fig 3), $\sigma_{2\%\text{-}OS}$ was slightly

more than 4 MPa. Table 2 shows stress at 1-mm deflection and 2% strain along with their offset values and COVs for all assemblies and ASTM samples. Variability in the data set decreased manyfold when 2% offset stress values were compared with $\sigma_{2\%\text{-}S}$. The 2% offset ($\sigma_{2\%\text{-}OS}$) is recommended as the $C_\perp$ strength value. This is the basis for further discussion.

Calculated stress values at all four deflection points, $\sigma_{0.04\text{-}D}$, $\sigma_{0.04\text{-}OD}$, $\sigma_{2\%\text{-}S}$, and $\sigma_{2\%\text{-}OS}$, are given in Table 2 along with their COVs for each assembly and their respective ASTM specimen. Mean stress at 2% offset strain ($\sigma_{2\%\text{-}OS}$) of all assemblies was significantly lower than corresponding ASTM tests of the main member (Table 2). For BC assemblies, ASTM values were lower than assembly values by 27-36%. Conversely, BP assemblies showed greater differences between the ASTM and assembly $\sigma_{2\%\text{-}OS}$ values. ASTM values for BP were higher than assembly values by 46 and 67% for DF and SPF, respectively. A possible reason for the general trend of higher ASTM values could be the opposite side longitudinal end bearing and wood-on-wood bearing of tested assemblies. Table 3 presents ratios of assembly performance to performance of corresponding ASTM tests of the main member based on mean $\sigma_{2\%\text{-}OS}$. Also shown are predicted ratios of assembly to ASTM test performance based on design procedures

Table 3. Ratio of assembly performance to corresponding ASTM test performance with predicted ratios from the literature.

Assembly[a]	Ratio assembly/ASTM (%)	Lum and Karacabeyli predicted (%)	Blass and Goerlacher predicted (%)
BC 2 × 4 DF	73	66	61
BC 2 × 4 SPF	69	66	61
BC 2 × 8 DF	78	66	61
BC 2 × 8 SPF	72	66	61
BC 2 × 12 DF	79	66	61
BC 2 × 12 SPF	75	66	61
BP DF	68	77	82
BP SPF	60	77	82

[a] BC, bottom chord; DF, Douglas-fir; SPF, spruce-pine-fir; BP, bottom plate.

proposed by Lum and Karacabeyli (1994) as well as Blass and Gorlacher (2004) and determined from the loading condition of the main member in each assembly. The design procedure proposed by Lum and Karacabeyli (1994) comes closer, in general, to predicting actual $\sigma_{2\%\text{-OS}}$ attained in testing. Each design procedure prediction was based on loading condition of the main member alone, ie the BC member. However, the TP members in BC assembly tests also contributed to the $C_\perp$ behavior of the assembly. TP members in the BC assembly would have a different predicted ratio and hence are likely contributors to some discrepancy between the theoretical and experimental ratios. Of all assembly tests performed, the BP assembly comes closest to idealizing the loading condition on which these ratios were predicted. In BP testing assemblies, the lower than predicted stress values achieved in testing were probably caused by nonparallelism of the specimens, which was mainly caused by the wood-on-wood contact involved in these assemblies (Fergus et al 1981).

Influence of Wood Species

Figure 4 shows the difference between mean $\sigma_{2\%\text{-OS}}$ for DF and SPF assemblies and corresponding 95% confidence intervals (CIs) based on pairwise comparisons. No statistically significant difference in $\sigma_{2\%\text{-OS}}$ was seen between DF and SPF BC tests (Fig 4a) even after accounting for covariates. The BC member dominated the
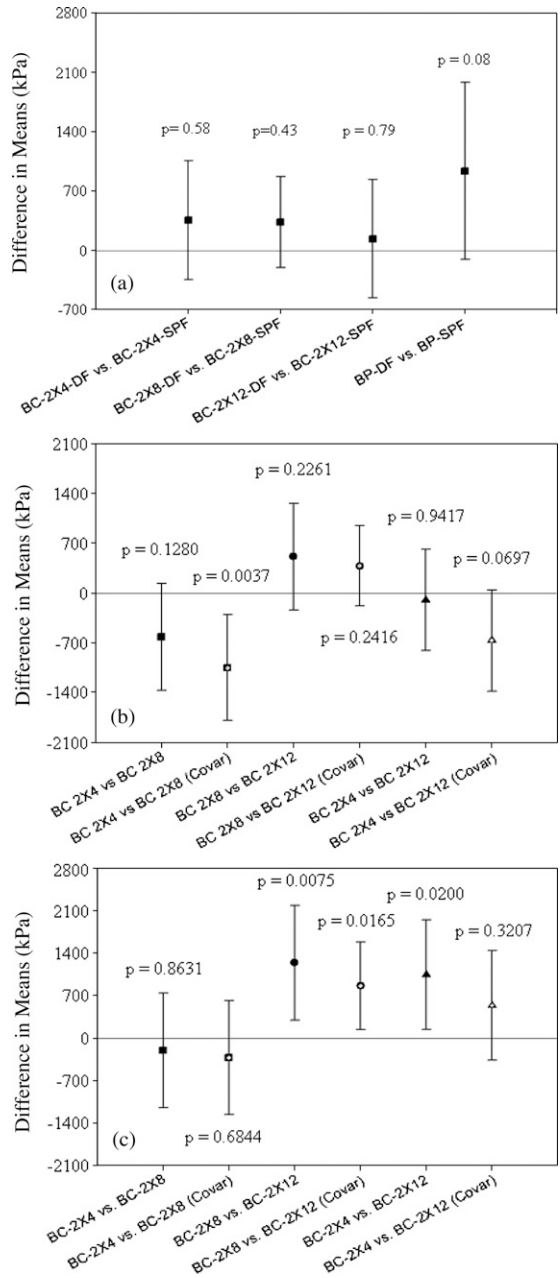

Figure 4. Tukey-Cramer multiple comparisons (a) all assemblies 95% confidence interval (CI) for difference in mean $\sigma_{2\%\text{-OS}}$; (b) bottom chord (BC) tests all 95% CI for difference in mean $\sigma_{2\%\text{-OS}}$ before and after accounting for covariate effect; (c) BC assemblies σ_{max} before and after adjustment for covariate effect.

$C_\perp$ behavior of BC assemblies. Because all BC members were DF, no significant difference in mean $\sigma_{2\%\text{-OS}}$ was observed between BC-DF and SPF assemblies. In BP assemblies, the BP main members were alternately DF and SPF in BP-DF and BP-SPF assemblies. As a result, there was suggestive but inconclusive evidence that mean $\sigma_{2\%\text{-OS}}$ of the BP-DF tests was 920 kPa ($p = 0.076$) more than that of BP-SPF assemblies. A significant difference in mean $\sigma_{2\%\text{-OS}}$ might have surfaced if more tests had been conducted. Bendtsen and Galligan (1979) statistically examined and analyzed the c-perp stress–strain relationship as well as the variability of this relationship for several softwood and hardwood species and found significant differences. Future studies are advised to have larger sample sizes to determine influence of wood species on BP assemblies.

Combined ASTM-DF tests showed significant differences ($p < 0.05$) compared with all test assemblies with DF main members (Table 2). ASTM-SPF tests showed significant differences compared with BP-SPF assemblies, because these were the only assemblies with SPF main members. ASTM tests were significantly different from corresponding test assemblies because loading conditions and contact surfaces were different. BC and BP test assemblies were loaded with opposite side end bearing in the main member, which is a more severe loading condition than that for ASTM $C_\perp$ (Lum and Karacabeyli 1994; Blass and Gorlacher 2004). Also, these members represented wood-on-wood bearing, which produces lower stresses than metal-on-wood bearing as in the ASTM $C_\perp$ specimen (Fergus et al 1981). When compared individually, ie one assembly compared with its corresponding ASTM specimens, differences in mean $\sigma_{2\%\text{-OS}}$ for all comparisons were also found to be statistically significant ($p < 0.05$). The only exception was BC-2 $\times$ 12-DF vs corresponding ASTM tests of the main member, which showed a suggestive but inconclusive difference ($p = 0.07$).

The ASTM $C_\perp$ specimen does not adequately represent main members in BC and BP assemblies. The ASTM $C_\perp$ specimen has limited appli-

cability to the opposite side end bearing condition of BC and BP assembly tests (Lum and Karacabeyli 1994; Blass and Gorlacher 2004; Leijten et al 2010). The wood-on-wood bearing in these assemblies further contributed to the lower stress value associated with BC and BP tests (Fergus et al 1981). It is therefore necessary to adjust from ASTM $C_\perp$ stress values to the $C_\perp$ stress values appropriate for these construction applications. This should include an adjustment factor for opposite side end bearing as well as an adjustment factor for wood-on-wood bearing.

Effect of Aspect Ratio on Performance

Because BC assemblies had three different aspect ratios, the discussion on effect of aspect ratio will focus on BC assemblies. However, as discussed previously, no significant differences in mean $\sigma_{2\%\text{-OS}}$ between BC-DF and BC-SPF assemblies were present. Therefore, BC-DF and BC-SPF tests were combined in Fig 4b. Mean $\sigma_{2\%\text{-OS}}$ of all BC tests was compared across assemblies. Based on 95% CI for specified linear combinations, no statistically significant difference in $\sigma_{2\%\text{-OS}}$ was seen among any BC assemblies before inclusion of covariate effects (ie all 95% CIs include 0). However, including covariate effects, the phenomenon changed (Fig 4b). Significant covariates in the model were average ring angle of the BC and specific gravity of both the TP and BC members (respective p values of 0.005 and 0.0185). After adjustment for covariate effect, mean $\sigma_{2\%\text{-OS}}$ of BC-2 $\times$ 4 tests was significantly lower than that of BC-2 $\times$ 8 tests ($p = 0.0037$). Mean stress of BC-2 $\times$ 4 tests was 1.02 MPa lower than that of BC-2 $\times$ 8 tests. There was also suggestive but inconclusive evidence that mean stress of BC-2 $\times$ 4 tests was lower than that of BC-2 $\times$ 12 tests ($p = 0.0697$). No significant difference in mean stress at 2% system offset strain was observed between BC-2 $\times$ 8 and BC-2 $\times$ 12 assembly tests.

These data suggest that mean values increased as aspect ratio increased from 2.3 for BC-2 $\times$ 4 assemblies to 4.8 for BC-2 $\times$ 8 assemblies. However, mean $\sigma_{2\%\text{-OS}}$ of BC-2 $\times$ 12 was not greater

than that of BC-2 × 8 members. As aspect ratio increased, the number of catastrophic failures increased, although there were no catastrophic failures observed for BC-2 × 4. Consequently, the increase in mean $\sigma_{2\%\text{-OS}}$ for BC-2 × 8 initially appeared to be counterintuitive given the fact that larger aspect ratios led to higher probability of catastrophic failure. However, most BC members in BC assemblies failed catastrophically only after attaining $\sigma_{2\%\text{-OS}}$. The greater $\sigma_{2\%\text{-OS}}$ in BC-2 × 8 compared with BC-2 × 4 assemblies is related to the stress distribution within BC members (Basta et al 2011). In BC members, the material to the outside of the region directly between top and bottom TP members provided support with corresponding strain in the material (Basta et al 2011) and was confirmed by finite element analysis (Basta 2005). This was more prominent for higher aspect ratio assemblies in finite element analyses (Basta 2005). Therefore, stress was distributed across a larger average cross-section in deeper members. Two × 8 BC members had stress distributed across a larger average cross-sectional area than did 2 × 4 BC members. Conversely, the mean $\sigma_{2\%\text{-OS}}$ of BC-2 × 12 was not greater than that of BC-2 × 8 members. The tendency of BC-2 × 12 members to buckle overshadowed the effect of increased depth of the members. When cross-grain bending occurred, this mode of compressive deflection dominated compressive behavior. Compressive deflection occurred predominantly through further cross-grain bending in the BC member rather than compressive deflection throughout the depth of the members (Basta et al 2011). Further study into the relationship between member depth and stress at specified strain in surface $C_\perp$ loading should be conducted.

Maximum Stress and Strain at Maximum Stress

Mean σ_{max} for the three BC assemblies was compared in Fig 4c. Species of TP material did not have a statistically significant impact on σ_{max} ($p = 0.36$; Fig 4c). Therefore, BC-DF and BC-SPF tests were combined. Similar to $\sigma_{2\%\text{-OS}}$, without covariate effects, no significant differences

in mean σ_{max} were present between BC-2 × 4 and BC-2 × 8 tests. However, both BC-2 × 4 and BC-2 × 8 tests have significantly different mean σ_{max} compared with BC-2 × 12 (respective p values of 0.02 and 0.0075). Mean σ_{max} of BC-2 × 4 and BC-2 × 8 was found to be 1.02 and 1.227 MPa, respectively, higher than that of BC-2 × 12. After adjusting for a significant covariate effect (ring angle, $p = 0.0199$), the difference in mean σ_{max} between BC-2 × 4 and BC-2 × 12 was no longer significant. However, the mean difference between BC-2 × 8 and BC-2 × 12 was estimated to be 850 kPa after adjustment for covariate effect and was significant ($p = 0.0165$). As explained previously, more support is provided by material away from the longitudinally loaded end of the BC member in deeper BC members. This could be responsible for the fact that BC-2 × 4 assemblies did not significantly outperform BC-2 × 12 assemblies based on σ_{max}. The significant difference in σ_{max} between BC-2 × 12 and BC-2 × 8 assemblies could have been caused by increased aspect ratio.

As the testing unfolded, analysis of the failure pattern showed that one BC-2 × 4-DF and BC-2 × 4-SPF test failed to reach the $F_{c\perp}$ listed in the NDS (AFPA 2007). In these two tests, the BC member was cut from near the pith and had annual rings with a low radius of curvature. These two BC members exhibited rolling shear along the earlywood/latewood interface combined with tension perpendicular to grain cracking. The majority of BC-2 × 4 and BC-2 × 8 assemblies reached σ_{max} values between 125 and 175% of $F_{c\perp}$. However, with increased aspect ratio of the BC member in BC-2 × 12 assemblies, six assemblies failed to reach F_c because of premature failure of the BC member. These failures were initiated by cross-grain bending in the BC member that resulted in rolling shear and tension perpendicular-to-grain damage with corresponding failure.

These data led to the conclusion that $C_\perp$ is a serviceability issue for lower aspect ratio members but may lead to a system stability issue in high aspect ratio members. Further research is necessary to develop a series of factors that will

adjust $C_\perp$ stress values from the ASTM specimen to appropriate stress values for applications in which load is applied to wood members with aspect ratios greater than 1. It is therefore recommended that further investigation is needed for the case of opposite side longitudinal end bearing in wood members through testing of different assemblies and species. In light of relatively recent changes in design codes, these data support the 2/3 reduction factor used in the Canadian design (Lum and Karacabeyli 1994) for $C_\perp$ when load is applied to opposite sides of a member near the longitudinal end of the member. However, this study does not agree as closely with Blass and Gorlacher (2004) and the German design approach in which allowable $C_\perp$ is based on full surface compression that is adjusted upward based on effective contact length parallel to grain. Standard dimensional lumber was used in this study, and these conclusions cannot be extrapolated to engineered wood products. Further studies are needed to establish the relationship between aspect ratio and $C_\perp$ behavior of engineered wood products.

CONCLUSIONS

To account for assembly depth, large settlement effect, and initial misalignment, a 2% offset strain method for determining and comparing stress values across differing assemblies and configurations as well as determining $C_\perp$ design values is recommended. Wood species did not have a significant influence on assembly performance. Mean stress at 2% offset strain of all assemblies was significantly lower than corresponding ASTM tests of the main member. The ASTM test does not adequately represent testing configurations in construction applications, and adjustment to design value is necessary for determining allowable $C_\perp$ stress values. However, more data are required to develop those adjustment factors. Aspect ratio affects $C_\perp$ behavior of wood members. $C_\perp$ has the potential to be a system stability issue in high aspect ratio members rather than a serviceability issue alone. Higher aspect ratios led to member instability because a 2×12 may fail catastrophically prior

to 2% system offset strain. The BC-2 $\times 12$ assemblies attained lower maximum stresses than the BC-2 $\times$ 8 assemblies. The 2×12 members may not have attained allowable stress values listed in the NDS.

REFERENCES

AFPA (2007) National design specification for wood construction. American Forest and Paper Association, Washington, DC.

ASTM (2010a) D 143-09. Standard methods for testing small clear specimens of timber. American Society for Testing and Materials, West Conshohocken, PA.

ASTM (2010b) D 2395-07. Standard test methods for specific gravity of wood and wood-based materials. American Society for Testing and Materials, West Conshohocken, PA.

Basta CT (2005) Characterizing perpendicular to grain compression in wood construction. MS thesis, Oregon State University, Corvallis, OR. 205 pp.

Basta CT, Gupta R, Leichti RJ, Sinha A (2011) Characterizing perpendicular to grain compression behavior in wood construction. Holzforschung 65:845-853.

Bendtsen BA, Galligan WL (1979) Modeling of the stress-compression relationship in wood in compression perpendicular to grain. Forest Prod J 29(2):42-48.

Blass HJ, Gorlacher IR (2004) Compression perpendicular to the grain. Pages 435-440 in Proc 8th World Conference of Timber Engineering, 14-17 June 2004, Lahiti, Finland. Finnish Association of Civil Engineers, Helsinki, Finland.

Bodig J (1969) Improved load-carrying capacity of wood in transverse compression. Forest Prod J 19(12):39-44.

Bulmanis NS, Latos HA, Keenan FJ (1983) Improving the bearing strength of light wood trusses. Can J Civil Eng 10:306-312.

Damkilde L, Hoffemeyer P, Pedersen TN (2000) Compression strength perpendicular to grain of structural timber and glulam. Holz Roh Werkst 58:73-80.

Fergus DA, Senft JF, Suddarth SK (1981) Recommended bearing stresses for design in light-frame construction. Forest Prod J 31(4):50-57.

Gehri E (1997) Timber in compression perpendicular to grain. Pages 355-374 in P Hoffmeyer, ed. Proc International Conference of IUFRO S5.02 Timber Engineering, 18-20 June 1997, Copenhagen, Denmark.

Johnson JW (1983) Compression perpendicular to the grain in dry Douglas-fir and hem-fir. Forest Prod J 33(3):55-63.

Kunesh RH (1968) Strength and elastic properties of wood in transverse compression. Forest Prod J 18(1):65-72.

Leijten AJM, Larsen HJ, Van der Put TACM (2010) Structural design for compression strength perpendicular to the grain of timber beams. Construct Build Mater 24:252-257.

Lum C, Karacabeyli E (1994) Development of the 'critical bearing' design clause in CSA-086.1. CIB Working

Commission (W18A)—Timber Structures in Sydney, Australia. Forintek Canada Corp., Vancouver, BC, Canada. 17 pp.

Lum C, Varoglue E (1988) Testing and analysis of parallel chord trusses. Pages 460-466 *in* Proc 1988 International Conference on Timber Engineering, Vol. 1. 19-22 September, Seattle, WA. University of Washington, Seattle, WA, Forest Products Research Society, Madison, WI.

Pellicane PJ, Bodig J, Mrema AL (1994a) Behavior of wood in transverse compression. J Test Eval 22(4):383-387.

Pellicane PJ, Bodig J, Mrema AL (1994b) Modeling wood in transverse compression. J Test Eval 22(4):376-382.

Ramsey FL, Schafer DW (2002) The statistical sleuth: A course in methods of data analysis. Duxbury/Thompson Learning, Pacific Grove, CA. 742 pp.

Schmidt RJ, Daniels CE (1999) Design considerations for mortise and tenon connections. Research Report, University of Wyoming, Department of Civil and Architectural Engineering, Laramie, WY. 98 pp.

Tibco Software Inc (2008) S plus 8.1 for Windows, New York, NY.

Wolfe RW, Percival DH, Moody RC (1986) Strength and stiffness of light-frame sloped trusses. Res Pap FPL-RP-471 USDA For Serv Forest Prod Lab, Madison, WI. 16 pp.